Electron Spin Resonance and Optical Studies of Poly(methylmethacrylate) Doped with $CuCl_2$

M. Abdelaziz

Department of Physics, Faculty of Science, Mansoura University, Mansoura 35516, Egypt

Received 11 February 2007; accepted 23 April 2007
DOI 10.1002/app.27320
Published online 22 January 2008 in Wiley InterScience (www.interscience.wiley.com).

ABSTRACT: Poly(methyl methacrylate) doped with $CuCl_2$ was prepared and its electron spin resonance (ESR) spectra and optical properties were studied. The ESR spectra can be accounted for by the presence of two radicals: R_a and R_b. FTIR spectroscopy reveals that there is no main difference of the spectra due to the addition of $CuCl_2$. The structural modifications are identified by investigating the doping level dependence of the peak heights of certain IR absorption peaks. The optical absorption, transmittance, and reflectance measurements were performed for prepared samples. The doping level (W) dependence on the g-factor (g), asymmetry factor (A), peak-to-peak separation (ΔH_{pp}), spin concentration (N), optical energy gap (E_{opt}), Urbach energy (E_u), refractive index (n), average oscillator wavelength (λ_o), and average oscillator strength (S_o) were estimated. It was found that these parameters are changed with doping level. These changes suggest high sensitivity of these films to doping that would suggest the applicability in magnetic and/or optical devices. © 2008 Wiley Periodicals, Inc. J Appl Polym Sci 108: 1013–1020, 2008

Key words: PMMA; $CuCl_2$; ESR; optical properties

INTRODUCTION

Poly(methyl methacrylate) (PMMA) is one of the best organic optical materials, and has been widely used to make a variety of optical devices. PMMA exhibits some specific properties such as an optical absorption in the visible domain, lighter weight, shock resistance, stable chemical property, good processibility, insulation character, simple synthesis, and low cost. One way to improve the properties of this polymer for optical applications is to form a charge transfer complex between the polymer and a dopant. The polymer is an electron donor and the dopant should be an electron acceptor.[1] It should be noted that formation of stable metal particles inside the polymer system is also of interest for potential applications such as 3D storage of optical data, shielding of electromagnetic radiation, flexible elements for resistive heating,[2] laser systems, polymer optical fiber amplifier, optical lenses, and integrated waveguides.[3]

Electron spin resonance (ESR) has been successfully applied to get information about transition metal ions in the polymer system. The ability to characterize the local structure of a paramagnetic center and sensitive detection of structural changes are given by ESR. Study of ESR and optical properties of transition metal ions in polymer matrix were applied to provide information on the structural properties of PMMA doped with $CuCl_2$ to moderate the magnetic and optical properties of PMMA films to form useful sensors and devices.

Correspondence to: M. Abdelaziz (mabdelaziz62@yahoo.com).

Journal of Applied Polymer Science, Vol. 108, 1013–1020 (2008)

EXPERIMENTAL

Sample preparation

PMMA with a low molecular weight, glass transition temperature of 105°C, and melting point of 225°C was provided by BDH Chemical, UK. Metal halide ($CuCl_2$) was supplied from Aldrich chemical company. PMMA doped with different concentrations of $CuCl_2$ were prepared by casting technique.[4] PMMA and $CuCl_2$ were dissolved in *N,N* dimethyacetamide for 3 days at 333 K. Certain amount of these dopant solutions were added to PMMA solution to obtain the concentrations: 0.0, 0.1, 0.5, 1.0, 2.5, 5.0, 7.5, and 10 wt %. The mixture was cast to a glass dish and kept in a dry atmosphere at 343 K for 2 weeks to minimize the solvent traces. The thickness of these films was in the range of 100–150 μm. The doping level W (wt %) was calculated from the following equation

$$W\ (\text{wt \%}) = \frac{W_d}{W_p + W_d} \times 100$$

where W_p and W_d represent the weight of polymer and dopant, respectively.

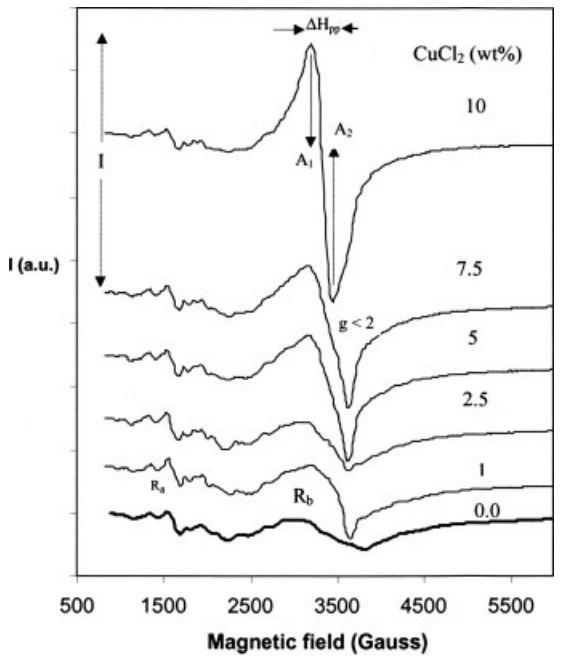

Figure 1 ESR spectra of different concentrations of $CuCl_2$ doped in PMMA.

Physical measurements

The ESR spectra were recorded on a JEOL spectrometer (type JES FE2XG) at a frequency of 9.45 GHz, using 1,*l*-diphenyl-2-picrylhydrazyl as a calibrant. The infrared spectrophotometer (Perkin-Elmer 833) was used for measuring the FTIR spectra in the wavenumber range 400–4000 cm^{-1}. UV–vis absorption spectra of the studied samples were carried out in the wavelength range of 200–900 nm using a Perkin-Elmer UV–vis spectrophotometer. The spectrophotometric method was used to determine the optical constants of the prepared films. The transmittance $T(\lambda)$ and the reflectance $R(\lambda)$ of the prepared films were measured using a double beam spectrophotometer JASCO model V-570-UV–vis–NIR. The transmittance and reflectance spectrum were measured at a wavelength of 900–2000 nm. A tungsten iodine lamp is used in the Vis/NIR region as light source.

RESULTS AND DISCUSSION

ESR

Figure 1 displays the obtained ESR signals for various $CuCl_2$-doped PMMA films. The observed signals are characterized by the following features. For undoped PMMA, the ESR spectrum can be accounted for by the presence of two radicals: R_a and R_b. R_a has a weak hyperfine line at about 1.5 kG, which is attributed to the main chain scission radical—$H_2C(^{\bullet})(COOMe)CH_3$. R_b has a broad single-line spectrum at $g = 2$. This broad single-line spectrum arose from coupling the unpair electron spin and a large number of protons.[5]

From the inset of Figure 1, it is evident that the individual lines of the radical R_a become weaker by increasing the content of $CuCl_2$, indicative of decreasing content of radical R_a. Furthermore, the broad single-line spectrum, attributed to radical R_b, becomes stronger and sharper by increasing $CuCl_2$ content. This peak is due to the aggregated form of the binuclear Cu^{2+} complex.[6]

The doping level, W, dependence of the dopant local structure can be clarified more explicitly with the aid of the peak-to-peak separation (ΔH_{pp}) of the main ESR Lorentzian signal, asymmetry factor ($A = A_1/A_2$), which is the ratio between the two halves of this signal and g-factor. The obtained values of ΔH_{pp}, A and g are plotted, as function of W, in Figure 2. It is clear that (i) a maximum g-factor (=2.032) value is noticed at doping level 0%. All the obtained g-values are smaller than 2, except for doping value of 10%, implying significant orbital contribution to the magnetic interaction. Maximum contribution is observed at doping level 1%. (ii) Asymmetry factor, A, has maximum value at doping level 2.5% and two minima at doping levels 1 and 5%. (iii) The behavior of ΔH_{pp} in the doping level range can be divided into three regions. In the first region, where the doping level ranges between 0 and 1%, ΔH_{pp} decreases steeply as W increases. In the second region, where the doping level ranges between 1 and 7.5%, ΔH_{pp} is nearly constant as W increases. In the third region, where the doping level ranges between 7.5% and 10%, ΔH_{pp} decreases as W increases. Accordingly, one may imply that the dipole interactions between the magnetic ions are randomly distributed in the amorphous regions of the polymeric matrix.

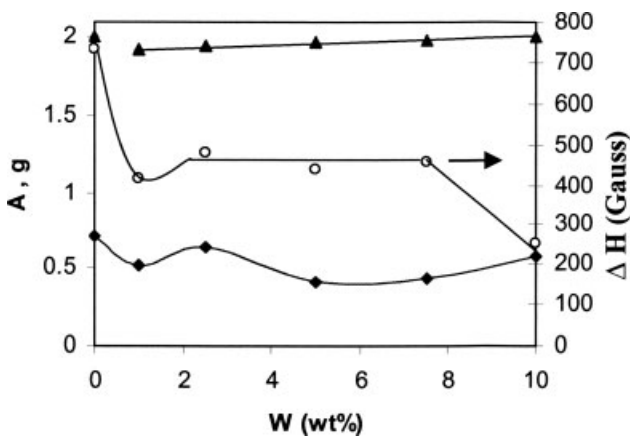

Figure 2 Doping level dependence of g (▲), A (■), and ΔH (○).

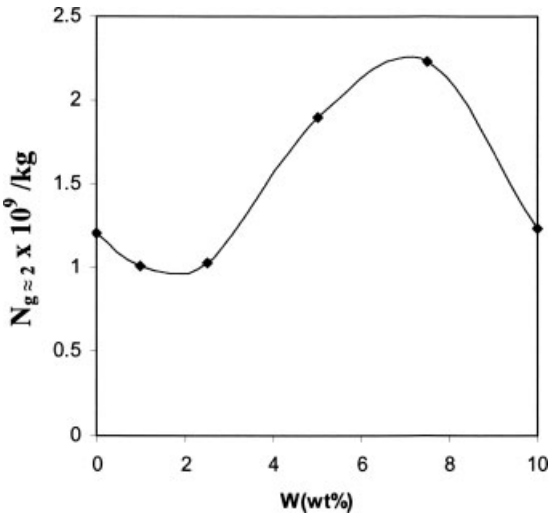

Figure 3 Doping level dependence of spin number concentrations.

Intensity and linewidth were estimated by relative peak-to-peak height (I) and width (ΔH_{pp}) in each first derivative resonance curve. The number of spins (N) participating in the resonance was roughly estimated by the equation[7]

$$N = I(\Delta H_{pp})^2. \quad (1)$$

The number of spins participating in resonance in this polymer system was calculated for different concentrations. Figure 3 shows a plot between the number of spins and doping level. It is clear that the spin concentration reveals a minimum spin content at doping level 1% and maximum spin content at doping level 7.5%.

FTIR spectroscopy

The influence of the addition of different concentrations of dopant to the polymeric films has been investigated by means of FTIR spectroscopy. Figure 4 shows the FTIR of the prepared films. The spectra are characterized by 3589, 3446, 2970, 2920, 1740, 1650, 1460, 1282, 1114, 985, and 755 cm^{-1}.

Romagnoli et al.[8] has reported that the appearance of two main peaks centered at about 3589 and 3446 cm^{-1}. These bands can be attributed to the vibration of free water OH groups and water H-bonded with carbonyl groups respectively. The vibrational frequencies at 2970 and 2920 cm^{-1} are assigned to O—CH_2 asymmetric stretching and CH_3 asymmetric stretching of PMMA. Two main bands are centered at 1740 and 1650 cm^{-1}, characterizing these spectra. The first band can be assigned to the combination of $\nu_{c=o}$ of carbonyl groups electrostatically interacting within the polymer chain and addition ions, while the second one is due to C=C bond.

Most single bonds absorb at frequencies between 1500 and 600 cm^{-1}. Nagai[9] has reported that the appearance of 985 cm^{-1} band is indicative to either atactic nature of PMMA. The vibrational peaks appearing in the range of 1000–600 cm^{-1} are assigned to C—H out-of-plane deformation. The absorption band at 755 cm^{-1} was assigned to rocking and wagging (CH_2). Other vibrational bands at 1114 and 1282 cm^{-1} are associated with the skeletal stretching which is coupled with C—H deformation vibration and arises from intermolecular interaction.[10]

A slight difference was present, for doped films, in the range 900–600 cm^{-1} that attributed to C—Cl stretching vibration, which leads us to believe that chlorination of the main chain occurs. The new bands may be correlated likewise to defects induced by the charge transfer reaction between the polymer chain and the dopant.[11] The structural disorder can be identified by investigating the doping level dependence of certain IR absorption peak. The peak height at 985 cm^{-1} is selected as an indicator for the structure deformations caused by the addition of $CuCl_2$. Figure 5 shows the doping level dependence of the intensity, I, of this peak. The curve exhibits two maxima at W = 0.1 and 2.5 wt % and minima at W = 1 wt %.

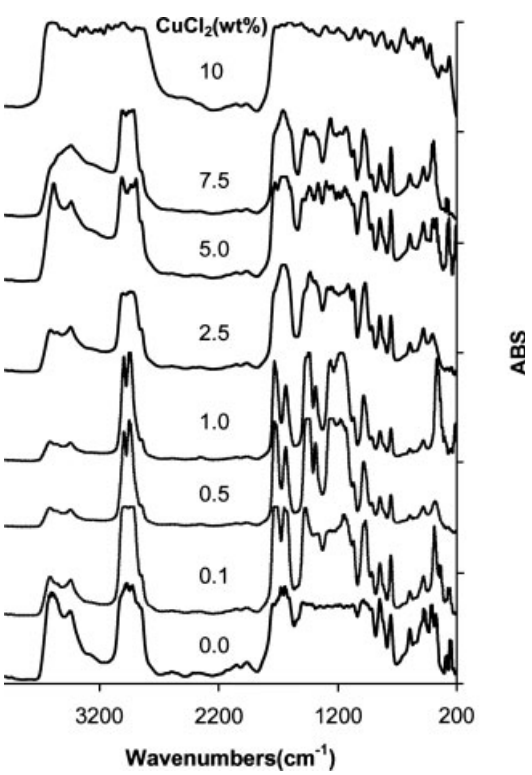

Figure 4 FTIR plots for PMMA doped with $CuCl_2$.

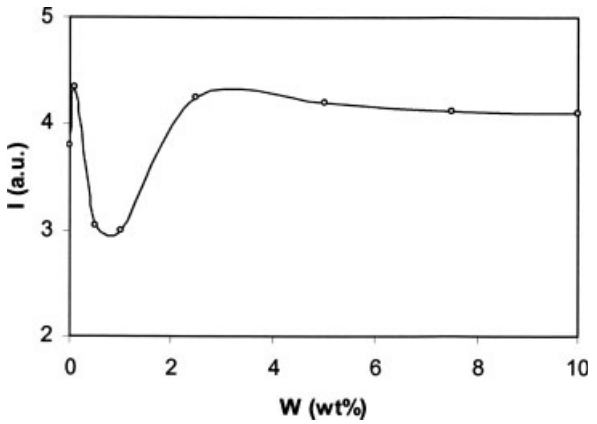

Figure 5 Doping level dependence of certain IR peak at 985 cm^{-1} for doped films.

Optical absorption spectra

The spectrum of the undoped PMMA shows a shoulder-like peak at about 260 nm which was assigned to the carbonyl group of PMMA.[12] Figure 6 reveals that the shoulder shifts toward the higher wavelengths and the absorption coefficient increases as doping level increases. This may be due to the increase of the number of carbonyl groups and strong interaction between PMMA and $CuCl_2$.

The spectra of doped films exhibit a valley of an increasing depth as $CuCl_2$ content increases. It is clear that the higher wavelength edge of the observed valley lies at $\sim$ 800 nm. This edge can be attributed to the Cu^{2+} absorption band,[13] which appears normally within the range of 690–800 nm which was assigned to the d–d band of Cu^{2+} due to the transition between ^2E and $^2T_2$ levels originating from the splitting of the ^2D ground states of the Cu^{2+} free ions d^9 in an octahedral field. Prakash and Rao[14] also observed a similar peak for Cu^{2+} ions in sodium fluoride–sodium borate glasses. Moreover, the five observed absorption bands in the UV range for $W = 7.5\%$ and 10% are probably charge-transfer-transition bands, because they arise from the higher lying energy levels. The present results indicate the presence of $CuCl_4^{2-}$ complexes. This result confirms with that obtained by ESR. Similar observations for Cu(II) complexes were reported by several studies.[15]

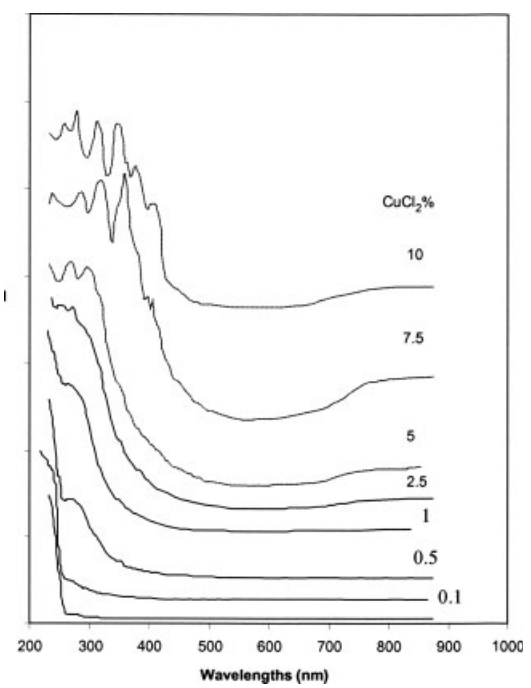

Figure 6 Room temperature optical absorption spectrum in the wavelength range (200–900 nm) for PMMA doped with $CuCl_2$.

Optical gap energy (E_{opt}) and Urbach energy (E_u)

The absorption of photons in a solid can occur for photon energies $h\nu \leq E_{opt}$ as well due to the presence of the tail states in the forbidden gap, which is usually close to the energy of the mobility edge. At low absorption levels, the absorption coefficient $\alpha(\nu)$ is described by the Urbach formula[16]

$$\alpha(\nu) = c \exp\left(\frac{h\nu}{E_u}\right) \quad (2)$$

where c is a constant dependent on the optical band gap but independent of photon energy $h\nu$ and E_u is called Urbach energy that is usually interpreted as the width of the tail of localized states in the forbidden band gap. The exponential dependence of $\alpha(\nu)$ on the $h\nu$ for the samples indicates that it obeys Urbach's rule. Figure 7 shows the Urbach plot for some samples with different concentration. The values of E_u are determined and plotted in Figure 8. A linear dependence of E_u on doping level is observed. As W increases, the values of E_u are found to be on

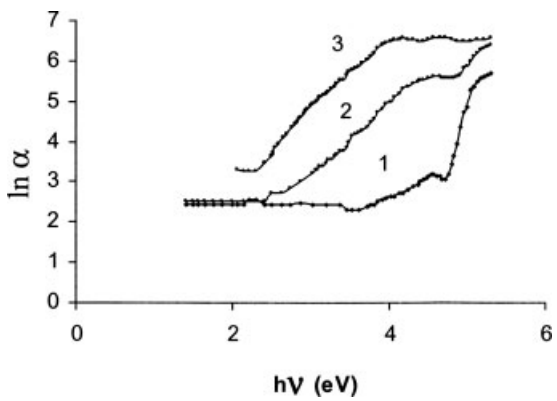

Figure 7 The dependence of natural logarithm of α on photon energy for (1) undoped, (2) 0.5%, (3) 5% $CuCl_2$.

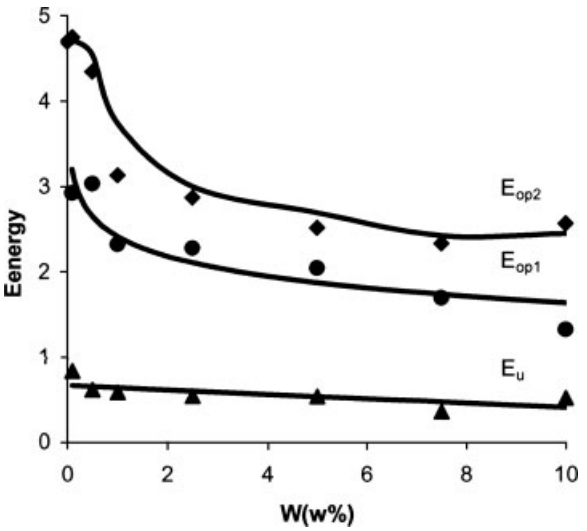

Figure 8 The dependence of $(\alpha h\nu)^{0.5}$ on photon energy for (1) undoped, (2) 0.5%, (3) 5% $CuCl_2$.

the decrease. The decrease of E_u in these samples can be understood by considering the mobility concept as proposed by Davis and Mott[17]; the dopant introduces additional defect states (e.g., color centers) in the polymeric matrix. The density of localized states was proportional to the concentration of these defects and consequently to dopant. Increasing $CuCl_2$ content may cause the localized states of the defects to overlap and extend the mobility gap. This overlap may give us evidence for increasing $CuCl_2$ content and the structural disorder is decreased in the polymeric matrix.

For optical transitions caused by photons of energy $h\nu > E_{opt}$, the density of both conduction and valence extended electronics states is assumed to depend on the square root of the energy, as found in a Fremi free-electron gas,[18–20] leading to an absorption coefficient, α, which depends on the photon energy as

$$\sqrt{\alpha h\nu} = \sqrt{B}[h\nu - E_{opt}] \quad (3)$$

where $\sqrt{B}$ is a proportional constant also known Tauc's constant and E_{opt} is defined as the energy band gap between the valence band and conduction band.

Plotting $\sqrt{\alpha h\nu}$ as a function of hν gives a straight line that is usually referred to as Tauc's plot. Extrapolation of the linear portion of these curves (see Fig. 9) gives the optical energy gap band E_{opt} for all prepared films. There are two optical energy band gaps E_{opt1} and E_{opt2}. The first one decreases as $CuCl_2$ content increases with numerical formula

$$E_{opt1} = -0.33 \ln W + 2.43 \quad (4)$$

where W is the doping level of $CuCl_2$ content. The second one has a valley behavior with minimum value at $W = 7.5\%$. These changes were argued by Akhter et al.[20] as first order process (carrier generation and recombination); or they may be due to some modifications in the size of the amorphous domains or platelets.

In other words, the decrease in an optical energy gap by doping may be explained on the basis of the fact that the incorporation of small amounts of dopant forms charge transfer complexes in the host lattice. The formation of charge transfer complexes in the polymer due to halogens introduces additional absorption bands in the UV and visible region of optical spectra.[21] Such absorption bands are observed in this study.

Optical constants

Optical constants (refractive index and the extinction coefficient) can be determined if the transmission and reflectivity measurements are made of the same sample. The spectral distribution of both transmittance $T(\lambda)$ and reflectance $R(\lambda)$ measured at normal incidence at room temperature for undoped PMMA and doped films in the wavelength range of 900–2000 nm are shown in Figure 10(a,b). It is clear that the undoped PMMA film is nearly transparent as $T + R = 1$. So there is no light is scattered or absorbed. On the other hand, for all the doped films the reflection increases and the transmission decreases to very small values. These films become colored, and most of the light is scattered or absorbed, that is, $T + R < 1$.

Neglecting multiple reflections and assuming that the film is perfectly smooth, calculations of the refractive index, n, and the extinction coefficient, k, from the absolute values of transmittance and reflectance have been performed by taking into account the experimental error in measuring both T and $R \pm$

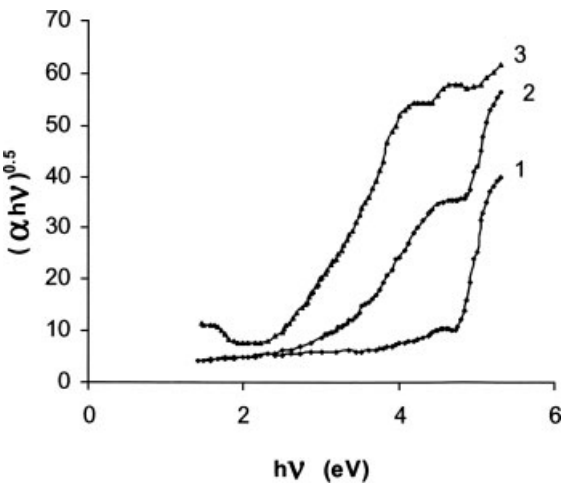

Figure 9 Doping level dependence of E_{opt1}, E_{opt2}, and E_u.

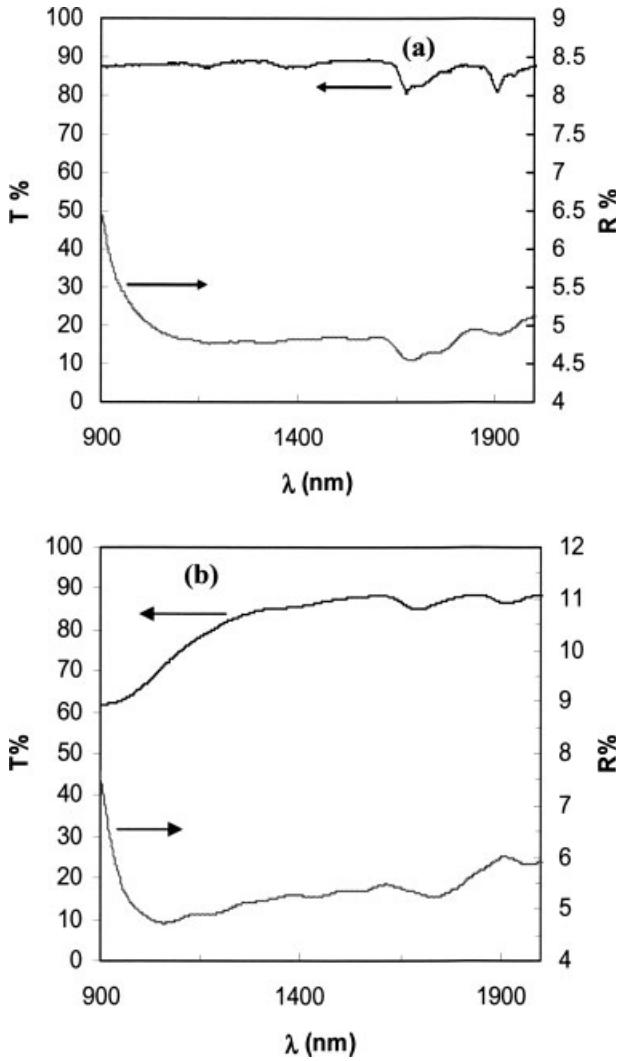

Figure 10 Variation in transmission and reflection with wavelength for (a) undoped PMMA and (b) PMMA doped 2.5% $CuCl_2$.

1%. The values of n for undoped and doped PMMA were determined from the measured values of $T(\lambda)$ and $R(\lambda)$ according to the following equations[22]

$$T(\lambda) = (1 - R)\ \exp\left(\frac{-4\pi kd}{\lambda}\right) \tag{5}$$

$$R(\lambda) = \frac{(n^2 - 1)^2 + k^2}{(n^2 + 1)^2 + k^2} \tag{6}$$

where d is the film thickness and $k = \alpha\lambda/4\pi$ is the extinction coefficient where α is the absorption coefficient. In the present work, the magnitude of n was adjusted using a computer aided program. Figure 11(a,b) shows the relation between n versus λ for undoped and doped PMMA. It is clear that the curve exhibits a monotonic decrease and then goes on nearly constantly at long wavelength suggesting a normal dispersion.

Figure 12 shows the dependence of the refractive index on doping level. It could be seen that the curve exhibits two maxima at doping levels 0.1% and 2.5% and minima at doping level 1%. It is remarkable that similar behavior is observed by IR analysis for absorption peak at 985 cm^{-1}. This indicates that the refractive indices are significantly influenced by atactic nature of PMMA doped with metal halide.

It is worth mentioning that the values of refractive indices for all films have nonmonotonic behavior. The change in the refractive index may be the result of the collection of dopant particles within the PMMA chain. On the other hand, the dopant remains uncomplexed like in the form of undissolved particles. This uncomplexed dopant must be responsible in reducing the refractive index of the mixture.[23]

The obtained values of the refractive index can be analyzed to yield the long wavelength refractive index (n_∞) together with the average interband oscillator wavelength (λ_o) and the average oscillator

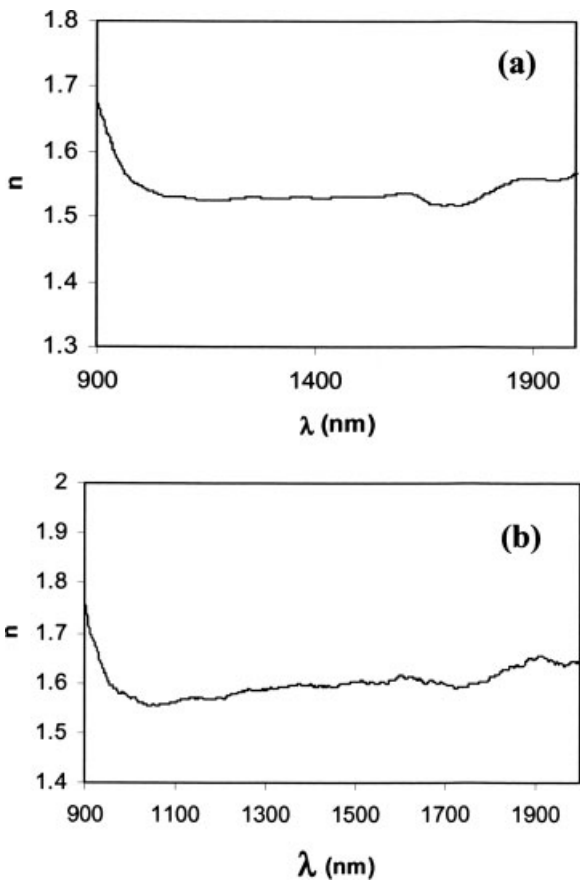

Figure 11 Dispersion curve of refractive index with wavelength for (a) undoped PMMA and (b) PMMA doped 2.5% $CuCl_2$.

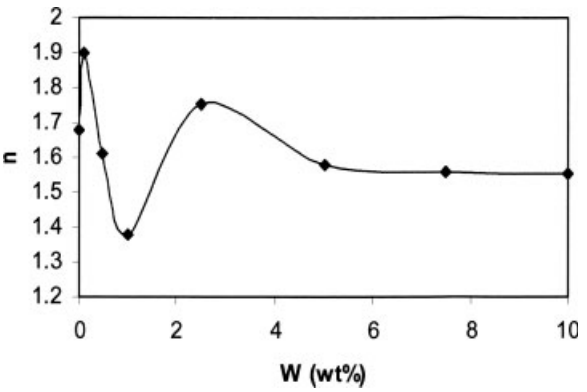

Figure 12 Doping level dependence of refractive indices.

strength (S_o) for the prepared films using the following equation

$$\frac{(n_\infty^2 - 1)}{(n^2 + 1)} = 1 - \left(\frac{\lambda_o}{\lambda}\right)^2 \tag{7}$$

where λ_o and n_∞ can be evaluated from plots of $(n^2-1)^{-1}$ against λ^{-2} as illustrated in Figure 13(a,b). Equation (7) can also be expressed as

$$(n^2 - 1) = \frac{s_o \lambda_o^2}{\left(1 - \frac{\lambda_o^2}{\lambda^2}\right)} \tag{8}$$

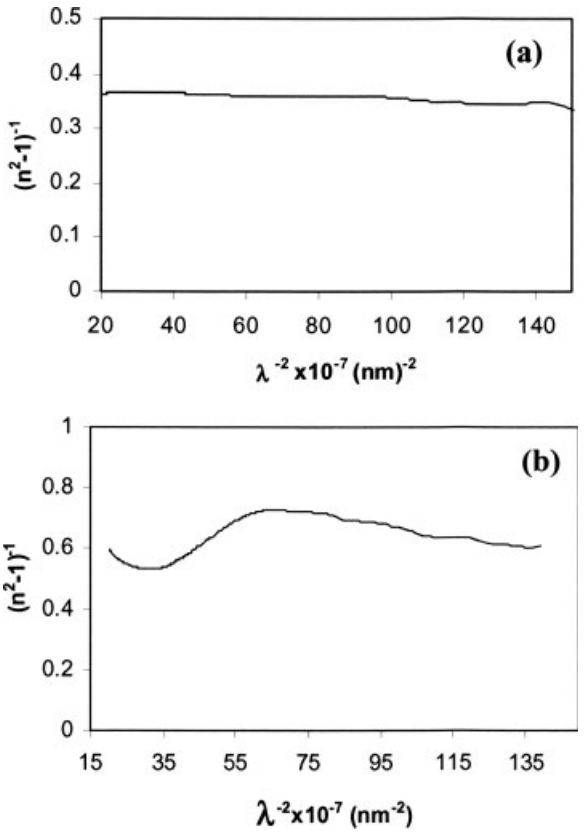

Figure 13 The plots of $(n^2-1)^{-1}$ against λ^{-2} for (a) undoped PMMA, (b) PMMA doped 2.5% $CuCl_2$.

TABLE I
The Doping Level Dependence of Optical Parameters

W (wt %)	S_o 10^{12}(nm)	λ_o (nm)	n_∞
Undoped	333	486	1.6
0.1	432	642	1.335
0.5	26	151	1.264
1.0	18	135	1.156
2.5	57	143	1.479
5.0	55	144	1.470
7.5	13	138	1.261
10	15	200	1.311

Average oscillator strength (S_o), average interband oscillator wavelength (λ_o), and long wavelength refractive index (n_∞).

where $S_o = (n_\infty^2 - 1)/\lambda_o^2$ is called the average oscillator strength. The values of the optical parameters S_o, λ_o, and n_∞ are listed in Table I. From this table, it is observed that the optical parameters change nonmonotonically by increasing the doping levels of $CuCl_2$. It may be said that the structural changes take place after doping with Cu as a result of complex formation of this additive with carbonyl group of PMMA with different modes depending on the doping levels. Thus it may be concluded that the doping is responsible for changing the refractive index of PMMA. According to recent works,[24,25] lower concentrations of the dopant may act as plastizeries, which increase the free volume among the polymer chains. These results suggest that it is possible to control the refractive index of polymeric films by type or/and doping level of the dopant.

CONCLUSIONS

The polymeric films of PMMA with different concentrations of $CuCl_2$ have been prepared and subjected to a detailed structural characterization and optical parameters as follows:

- ESR spectra indicate that there are two types of radicals R_a and R_b in undoped and doped PMMA. R_a decreases while R_b increases as $CuCl_2$ increases.
- FTIR spectra suggest a structural change after doping with $CuCl_2$ as results of complex formation of Cu with carbonyl group of PMMA.
- The optical absorption measurements indicate that the absorption mechanism is due to indirect transition. Optical energy gaps (E_{opt}) have a monotonic decrease as doping level increases while a linear decreasing of Urbach energies (E_u) are observed for prepared films. The reduced values of the optical gaps, obtained for doped films improve their optical response. These films can be used as microwave sensors.

- The optical parameters S_o, λ_o, and n_∞ are summarized in Table I. Nonmonotonic behaviors are observed. We believe that this change in the refractive index by doping level could lead to usage of these films in optical switching devices such as gratings or waveguides.

References

1. Tauihri, S.; Bernede, J. C.; Molinie, P.; Legoff, D. Polymer 2002, 43, 3123.
2. Mills, G.; Slaten, N.; Broughton R., Annual report (Photoadaptive fibers for textile materials), Nov. 1999, M98–A10.
3. Kumar, G. A.; Martinez, A.; Elder De La Rosa. J Lumin 2002, 99, 141.
4. Abdelaziz, M. Effect of filling with mixed transition metal chlorides on the physical properties of polyvinylidene fluoride and some of its blends. PhD Thesis; Mansoura University: Egypt, 2002.
5. Shany Lin, Y.; Lee, J.; Cheng, C. P. Mater Chem Phys 2003, 78, 847.
6. El-khodray, A.; Abdelaziz, M.; Hassan, G. M. Int J Polym Mater 2005, 54, 633.
7. Rao, J. L.; Murali, A.; Rao, E. D. J Non-Cryst Solids 1996, 202, 215.
8. Romagnoli, P.; Trombetta, M.; Licoccia, S. J Eur Ceram Soc 2004, 24, 1153.
9. Nagai, H. J Appl Polym Sci 1963, 7, 1697.
10. Kelkar, D. S.; Gader A. P. J Appl Polym Sci 1998, 70, 1627.
11. Zhan, X.; Xu, S.; Yang, M.; Shen, Y.; Wan, M. Eur Polym J 2002, 38, 2057.
12. Zidan, H. M.; Tawansi, A.; Abu-Elnader, M. Phys B 2003, 339, 78.
13. Tawansi, A.; Oraby, A. H.; Bader, S. I.; Abdelaziz, M. J Mater Sci Mater Electron 2003, 14, 135.
14. Prakash, P. G.; Rao J. L. J Mater Sci 2004, 39, 193.
15. Shinde, S. S.; Dhabekar, B. S.; Gundu, T. K.; Bhatt, B. C. J Phys D: Appl Phys 2001, 34, 2683.
16. Urbach, F. Phys Rev 1953, 92, 1324.
17. Davis, E. A.; Mott, N. Philos Mag 1970, 22, 903.
18. Aydogdu, Y.; Yakuphanoglu, F.; Aydogdu, A.; Tas, E.; Cukuraval, A. Solid State Sci 2002, 4, 879.
19. Aydogdu, Y.; Yakuphanogul, F.; Aydogdu, A.; Sekerci, M.; Balci, Y.; Aksoy, I. Synth Met 1999, 107, 191.
20. Akhter, M.; Pramanik, P.; Biswas, M. J Polym Sci Part B 1987, 25, 339.
21. Raja, V.; Sarma, A. K.; Narasimha Rao, V. V. R. Mater Lett 2003, 57, 4678.
22. Soliman, H. S.; El-Kadry, N.; Gamjoum, O.; El-Nahass, M. M.; Darwish, H. J Opt 1988, 17, 46.
23. Kellkar, D. S.; Gadre, A. P. J Appl Polym Sci 1998, 70, 1627.
24. Tang, B. Z.; Leung, S. M.; Peng, H.; Yu, N. T.; Su, K. C. Macromolecules 1997, 30, 2848.
25. Mansour, A. F. Int J Polym Mater 2005, 54, 227.